Supporting Information

For

ATR-FTIR spectroscopy supported by multivariate analysis for the characterization of adipose tissue aspirates from patients affected by systemic amyloidosis.

Diletta Ami[$], Paolo Mereghetti[$], Andrea Foli[§], Masayoshi Tasaki[§#], Paolo Milani[§], Mario Nuvolone[§], Giovanni Palladini[§], Giampaolo Merlini[§], Francesca Lavatelli[§]*, Antonino Natalello[$]*

$Department of Biotechnology and Biosciences, University of Milano-Bicocca, Piazza della Scienza 2, 20126 Milano, Italy.

§Amyloidosis Research and Treatment Center, Fondazione IRCCS Policlinico San Matteo and Department of Molecular Medicine, University of Pavia, Viale Golgi 19, 27100, Pavia, Italy.

Department of Morphological and Physiological Sciences, Graduate School of Health Sciences, Kumamoto University, 4-24-1 Kuhonji, Kumamoto 862-0976, Japan, and Department of Neurology, Graduate School of Medical Sciences, Kumamoto University, 1-1-1 Honjo, Kumamoto 860-0811, Japan.

Corresponding Authors

* Antonino Natalello, Email: antonino.natalello@unimib.it

* Francesca Lavatelli, Email: francesca.lavatelli@unipv.it

Content: two supporting tables and six supporting figures.

Code	Age (years), gender	CR score*	Systemic amyloidosis type	Diagnosis **
Individuals affected by systemic amyloidosis				
1	68, M	1+	AL λ	AL amyloidosis with kidney involvement
2	72, M	2+	AL κ	AL amyloidosis with kidney involvement
3	74, M	2+	AL λ	MM with amyloid deposition in fat, no organ involvement
4	67, F	4+	AL λ	AL amyloidosis with kidney involvement
5	56, M	3+	AL λ	AL amyloidosis with heart and soft tissues involvement
6	62, F	4+	AA	AA amyloidosis with kidney involvement
7	62, F	3+	AL λ	AL amyloidosis with heart and soft tissues involvement
8	70, F	4+	AL λ	AL amyloidosis with kidney involvement
9	71, M	3+	AL λ	MM with amyloid deposition in fat, carpal tunnel syndrome
10	79, M	3+	AL λ	AL amyloidosis with heart involvement
11	59, F	3+	AL κ	AL amyloidosis with heart, kidney and liver involvement
Individuals not affected by systemic amyloidosis				
1	75, M	0	-	Amyloidoma of the spine
2	56, F	0	-	Localized amyloidosis (larynx)
3	59, M	0	-	MGUS IgAλ (normal κ/λ FLC ratio)
4	72, F	0	-	Hypertensive cardiomyopathy, no amyloidosis
5	65, M	0	-	MGUS IgMλ (normal κ/λ FLC ratio)
6	75, M	0	-	Localized amyloidosis (palate)
7	74, M	0	-	Localized amyloidosis (skin nodule)
8	44, M	0	-	Chronic inflammatory demyelinating polyneuropathy, no amyloidosis
9	71, M	0	-	Localized amyloidosis (lung nodule)
10	89, M	0	-	Suspected intestinal amyloidosis, not confirmed by histology
11	52, F	0	-	Localized amyloidosis (eye socket)
12	49, M	0	-	Localized amyloidosis (eyelids)
13	54, M	0	-	Chronic inflammatory demyelinating polyneuropathy, no amyloidosis

Table S-1. Main clinical and pathologic features of the individuals included in the study.
Abbreviations: FLC: Free Light Chains; M: Male; F: Female; CR: Congo Red; MM: Multiple Myeloma; MGUS: Monoclonal Gammopathy of Undetermined Significance.

*as described in Van Gameren et al. 2010 [12].
** Clinical characterization was performed as previously described [4]. Amyloid organ involvement in AL amyloidosis was defined according to Gertz et al. 2015 [13].

Method	Absorption spectra / Second derivatives	Spectral range (cm^{-1})	AUC (%)	Sensitivity (%)	Specificity (%)
xgbTree	Absorption spectra	3050-2800	58	53	54
		1700-1500	80	74	78
		1700-1200	85	75	72
		1500-1200	82	73	72
MARS	Absorption spectra	3050-2800	66	65	76
		1700-1500	77	80	89
		1700-1200	80	83	93
		1500-1200	81	80	90
PLS-DA	Absorption spectra	3050-2800	86	85	82
		1700-1500	93	97	81
		1700-1200	94	94	88
		1500-1200	91	91	86
xgbTree	Second derivatives	3050-2800	85	75	77
		1700-1500	93	85	85
		1700-1200	93	77	88
		1500-1200	91	75	85
MARS	Second derivatives	3050-2800	80	73	81
		1700-1500	91	88	87
		1700-1200	98	84	85
		1500-1200	88	83	87
PLS-DA	Second derivatives	3050-2800	88	87	90
		1700-1500	**99**	**100**	**90**
		1700-1200	**97**	**100**	**100**
		1500-1200	93	87	90

Table S-2. Overall discrimination performance of the tested chemometrics analyses.
Four spectral regions (3050-2800 cm^{-1}, 1700-1500 cm^{-1}, 1500-1200 cm^{-1}, and 1700-1200 cm^{-1}) were tested. The analysis was performed using absorption spectra and second derivatives. For each condition the median (over the 10-time repeated 5-fold cross-validation) area under the curve (AUC), sensitivity and specificity are reported.
Values ≥ 90% are highlighted in yellow. The more performing approaches are indicated in red text.

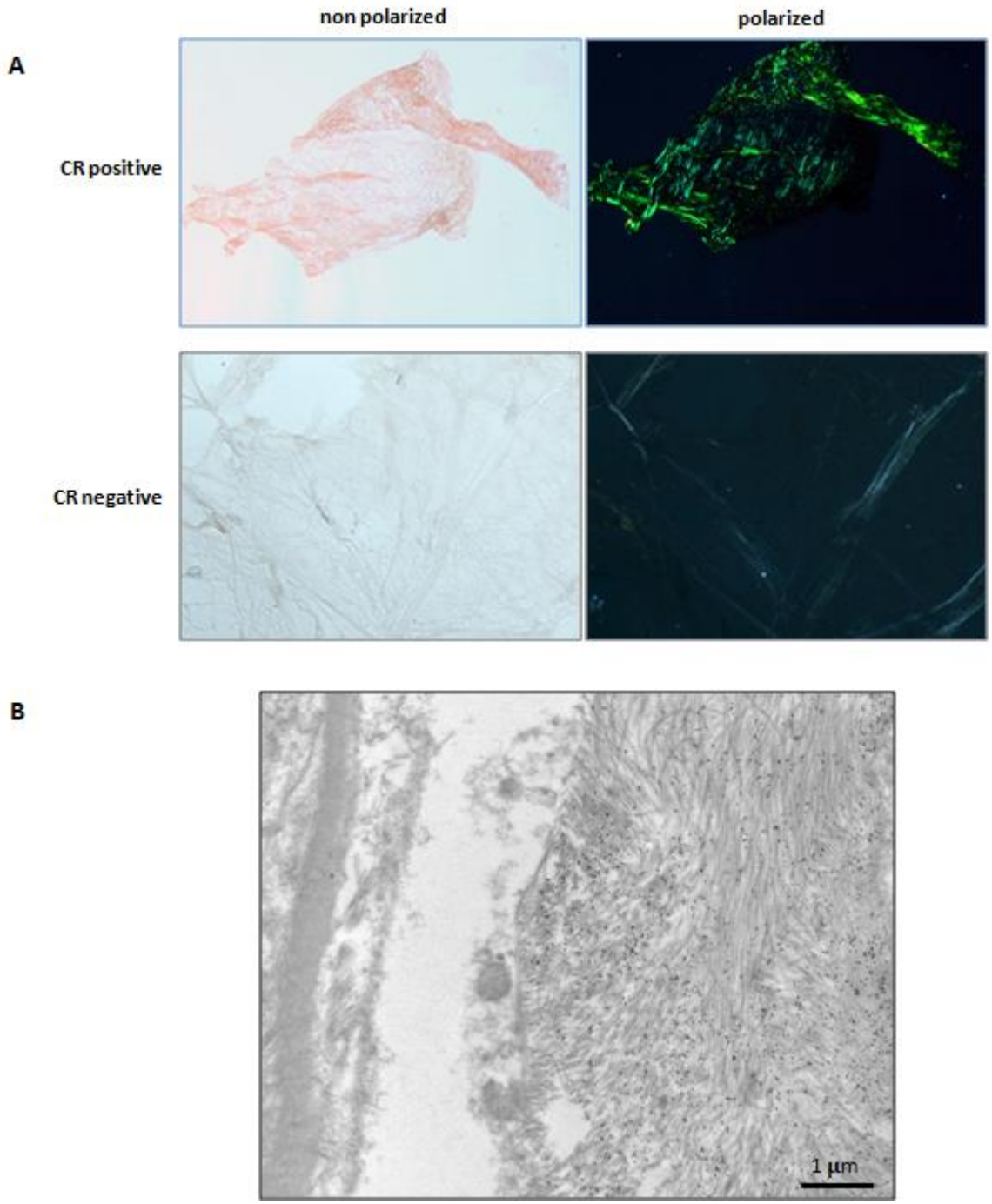

Figure S-1: (A) Representative Congo red (CR) negative and positive adipose tissue aspirates visualized under non polarized (left panels) and polarized light (right panels). Amyloid-positive regions appear as apple-green areas. (B) Representative immuno elecron microscopy analysis of abdominal fat aspirates from a patient affected by AL κ systemic amyloidosis. Postembedding immunostaining with polyclonal anti-κ light chains antibodies (Dako, Agilent Technologies, CA, USA). Secondary antibodies are conjugated with gold particles (black dots). Immunogold labeled amyloid fibrils are visible in right side of the figure.

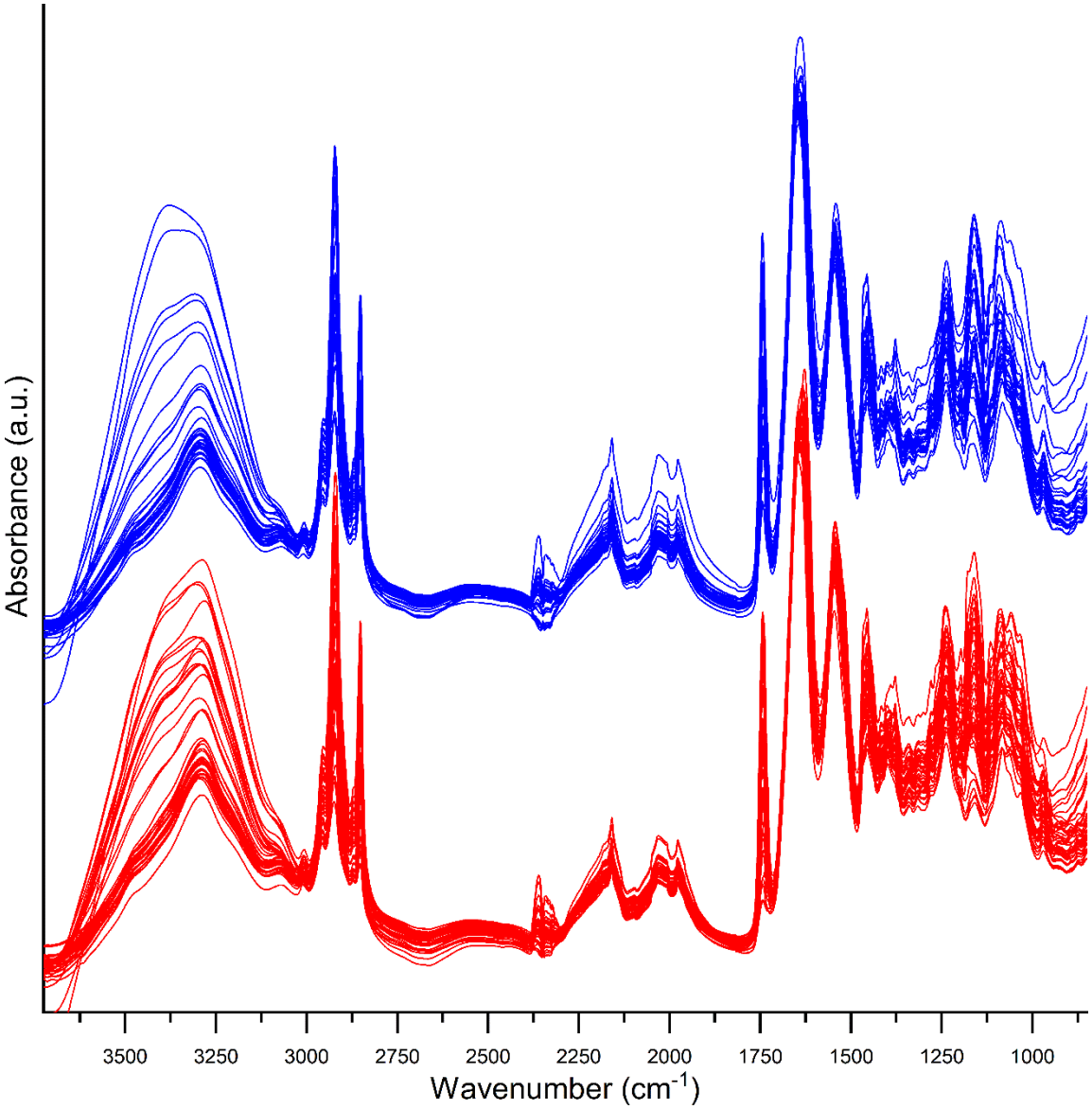

Figure S-2: Measured ATR-FTIR absorption spectra. Absorption spectra from amyloid-positive individuals (red) and from CR-negative controls (blue) are reported without baseline correction and before smoothing. For better visualization, spectra are showed after normalization at the Amide I band area and shifted in the Y axis. The signal in the 2500-1950 cm^{-1} spectral region is affected by the diamond absorption of the ATR device.

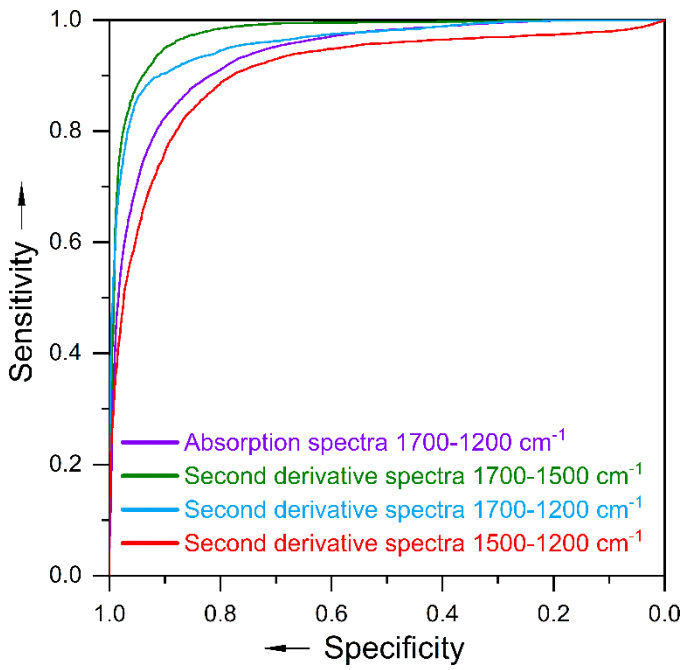

Figure S-3. Representative ROC curves. ROC curves are shown for four representative conditions: PLS-DA, absorption spectra, range 1700-1200 cm^{-1}; PLS-DA, second derivatives, range 1700-1500 cm^{-1}; PLS-DA, second derivatives, range 1700-1200 cm^{-1}; PLS-DA, second derivatives, range 1500-1200 cm^{-1}. Each ROC curve is an average (mean) of 50 ROC curves obtained by the 10-time repeated 5-fold cross-validation training procedure.

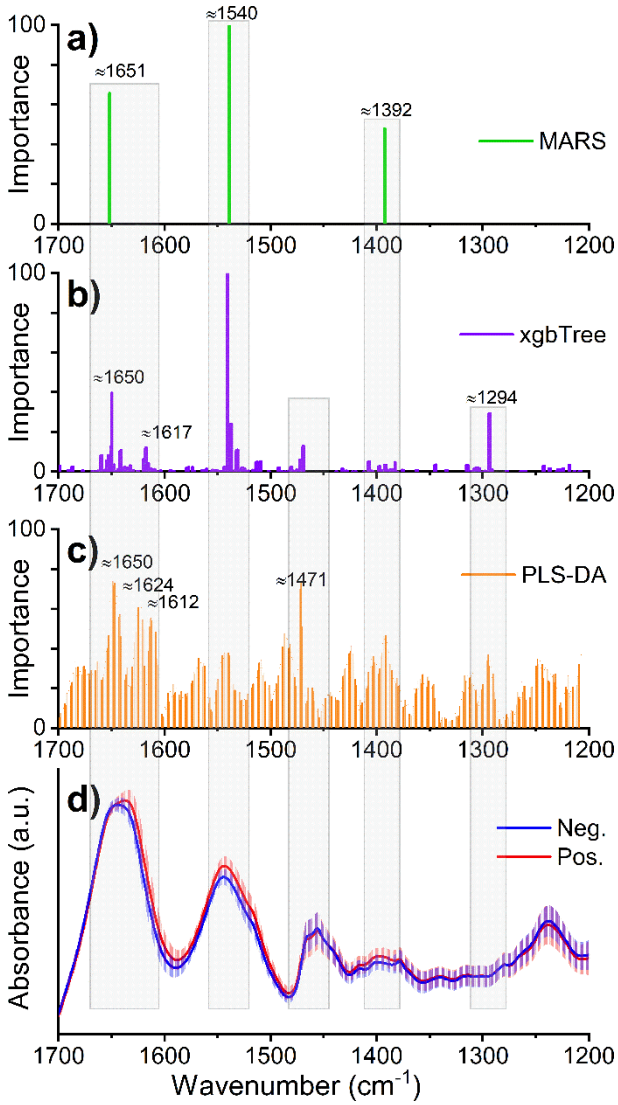

Figure S-4. Wavenumber importance profiles obtained from the MARS (a), xgbTree (b) and PLS-DA (c) methods performed on the ATR-FTIR absorption spectra in the 1700-1200 cm^{-1} region. The average absorption spectra of CR-positive (Pos.) and CR-negative (Neg.) individuals are also reported (d) for comparison. Error bars represent the standard deviations. Relevant components are indicated.

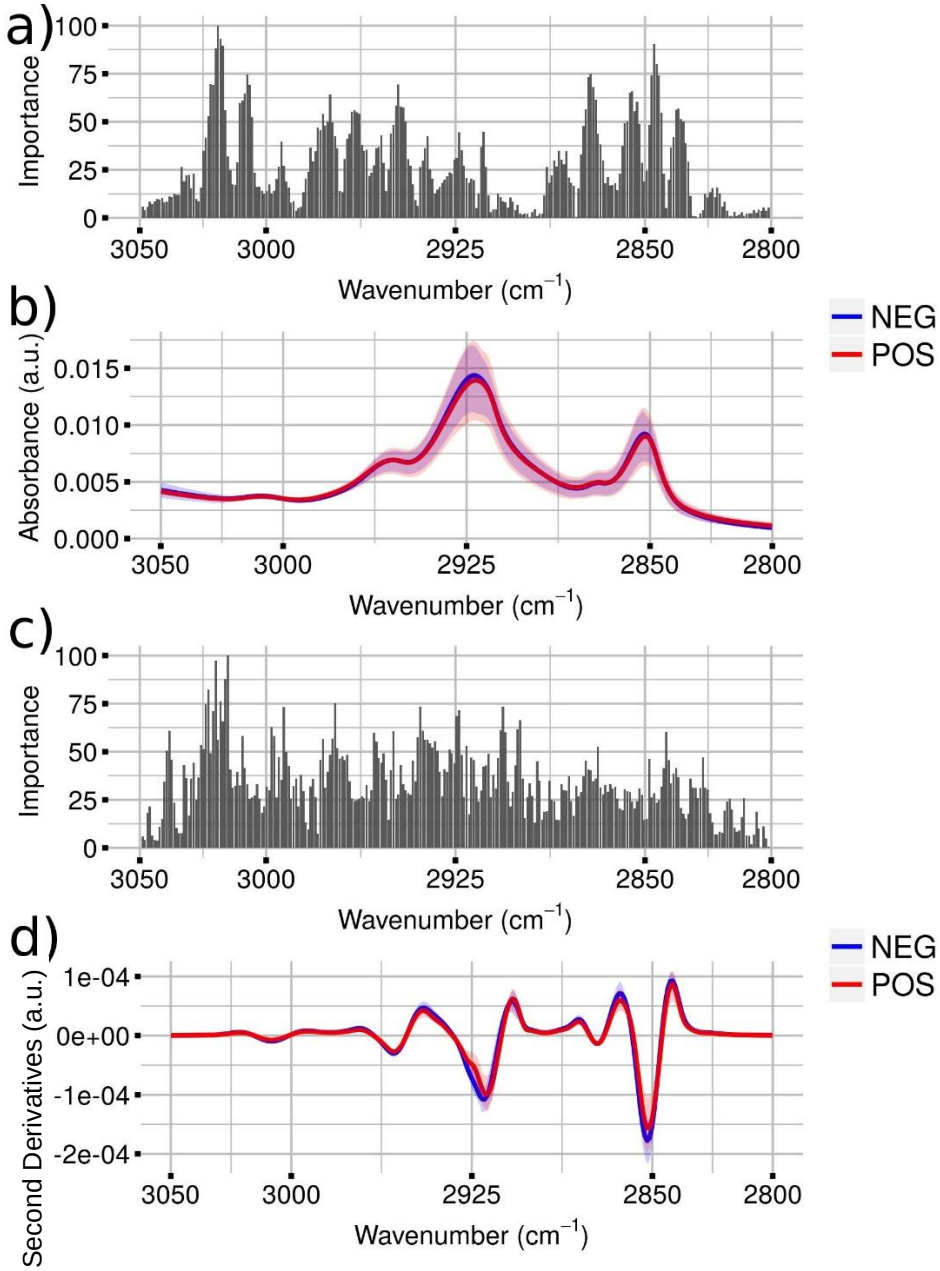

Figure S-5. Wavenumber importance profiles obtained from the PLS-DA method performed on the ATR-FTIR absorption and second derivative spectra in the 3050-2800 cm^{-1} range. (a) Wavenumber importance (domain 0-100) for PLS-DA discrimination performed in the 3050-2800 cm^{-1} spectral region obtained from the analysis of the ATR-FTIR absorption spectra. (b) Average absorption spectra of CR-positive (POS) and CR-negative (NEG) individuals. Shaded areas represent the standard deviations. (c) Wavenumber importance (domain 0-100) for PLS-DA discrimination performed in the 3500-2800 cm^{-1} spectral region obtained from the analysis of the second derivatives of the ATR-FTIR absorption spectra. (d) Average second derivative spectra of CR-positive (POS) and CR-negative (NEG) individuals. Shaded areas represent the standard deviations.

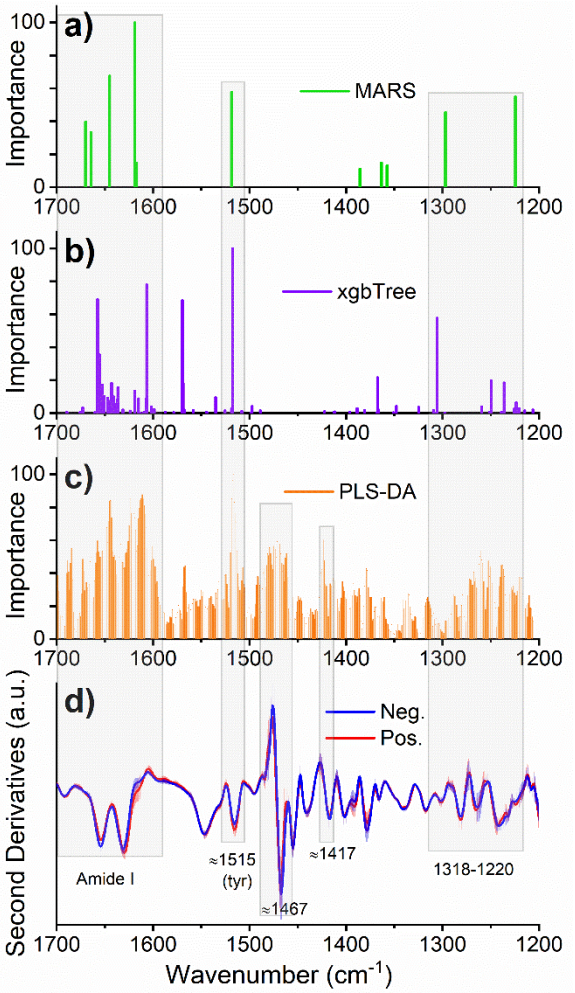

e) Second derivative spectra		
Peak (cm^{-1})	**Assignment**	**References**
~1654	protein α-helical and random coil structures	15, 27
~1630	protein β-sheets	15, 27
~1616	protein intermolecular β-sheets, amino acid side chains	14, 15, 27, 35, 36
~1515	tyrosine	29
~1467	mainly hydrocarbon chain CH_2 groups	28,37
~1417	mainly hydrocarbon chain CH_2 groups	39
~1318-1220	protein Amide III band, phospholipid phosphate moiety, hydrocarbon chain CH_2 groups and other biomolecules.	26, 27, 28, 39

Figure S-6. Wavenumber importance profiles obtained from the MARS (a), xgbTree (b) and PLS-DA (c) methods performed on the ATR-FTIR second derivate spectra in the 1700-1200 cm^{-1} region. The average second derivative spectra of CR-positive (Pos.) and CR-negative (Neg.) individuals are also reported (d) for comparison. Error bars represent the standard deviations. Relevant components are indicated. (e) Assignment of the most significant peaks of the second derivative spectra.